AD-A043 118 KENTUCKY UNIV LEXINGTON DEPT OF ENGINEERING MECHANICS F/G 21/5
THERMO-MECHANICAL STRESS ANALYSIS OF ADVANCED TURBINE BLADE COO--ETC(U)
JUL 77 F J RIZZO, D J SHIPPY AF-AFOSR-2824-75
UNCLASSIFIED UKY-TR104-77-EM15 AFOSR-TR-77-0950 NL

1 OF 1
ADA043118

END
DATE FILMED
9-77
DDC

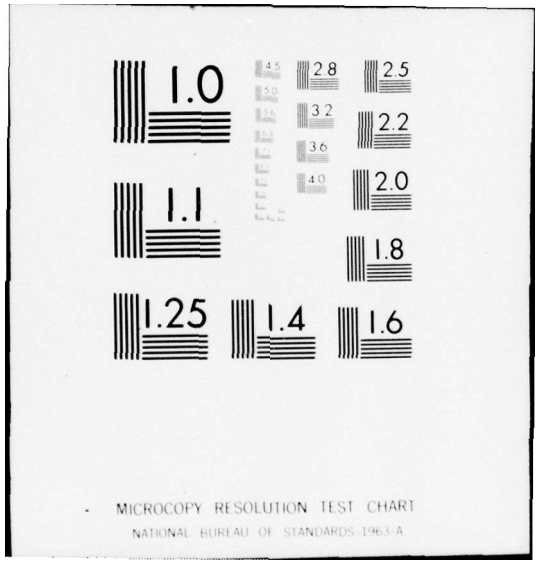
1.0
1.1
1.25
1.4
1.6
1.8
2.0
2.2
2.5
2.8
3.2
3.6
4.0
4.5
5.0
5.6
MICROCOPY RESOLUTION TEST CHART
NATIONAL BUREAU OF STANDARDS 1963-A

AFOSR-TR-77-0950

AFOSR

UKY-TR104-77-EM15
July 1977

THERMO-MECHANICAL STRESS ANALYSIS OF ADVANCED TURBINE BLADE COOLING CONFIGURATION

INTERIM SCIENTIFIC REPORT, 1 May 76 - 31 June 77

F. J. Rizzo & D. J. Shippy
Department of Engineering Mechanics
University of Kentucky
Lexington, Kentucky 40506

2307
AI
July 1977
49p.

Interim Report for Period 1 May 1976 through 30 June 1977

AF-AFOSR-2824-75

Approved for Public Release
Distribution Unlimited

Prepared For
Air Force Office of Scientific Research
Bolling Air Force Base
Washington, D.C. 20332

403 077

SECURITY CLASSIFICATION OF THIS PAGE (When Data Entered)

REPORT DOCUMENTATION PAGE		READ INSTRUCTIONS BEFORE COMPLETING FORM
1. REPORT NUMBER AFOSR-TR- 77-0950	2. GOVT ACCESSION NO.	3. RECIPIENT'S CATALOG NUMBER
4. TITLE (and Subtitle) THERMO-MECHANICAL STRESS ANALYSIS OF ADVANCED TURBINE BLADE COOLING CONFIGURATION		5. TYPE OF REPORT & PERIOD COVERED INTERIM 1 May 1976 - 30 June 1977
		6. PERFORMING ORG. REPORT NUMBER UKY TR104-77-EM15
7. AUTHOR(s) F. J. RIZZO D. J. SHIPPY		8. CONTRACT OR GRANT NUMBER(s) AFOSR-75-2824
9. PERFORMING ORGANIZATION NAME AND ADDRESS UNIVERSITY OF KENTUCKY DEPARTMENT OF ENGINEERING MECHANICS LEXINGTON, KENTUCKY 40506		10. PROGRAM ELEMENT, PROJECT, TASK AREA & WORK UNIT NUMBERS 2307B1 61102F
11. CONTROLLING OFFICE NAME AND ADDRESS AIR FORCE OFFICE OF SCIENTIFIC RESEARCH/NA BUILDING 410 BOLLING AIR FORCE BASE, D.C. 20332		12. REPORT DATE July 1977 13. NUMBER OF PAGES 36
14. MONITORING AGENCY NAME & ADDRESS(if different from Controlling Office)		15. SECURITY CLASS. (of this report) UNCLASSIFIED 15a. DECLASSIFICATION/DOWNGRADING SCHEDULE

16. DISTRIBUTION STATEMENT (of this Report)

Approved for public release; distribution unlimited

17. DISTRIBUTION STATEMENT (of the abstract entered in Block 20, if different from Report)

18. SUPPLEMENTARY NOTES

19. KEY WORDS (Continue on reverse side if necessary and identify by block number)

BOUNDARY INTEGRAL EQUATION METHOD
THERMO-MECHANICAL STRESS ANALYSIS
STRESS CONCENTRATION
TURBINE BLADE COOLING HOLE

20. ABSTRACT (Continue on reverse side if necessary and identify by block number)

Program improvement features in a Boundary Integral Equation Analysis Capability for thermomechanical problems are described. A number of solved problems are presented along with a progress report on the research directed toward a thermomechanical stress analysis in the vicinity of a cooling hole in a film-cooled turbine blade.

DD FORM 1 JAN 73 1473 EDITION OF 1 NOV 65 IS OBSOLETE UNCLASSIFIED

SECURITY CLASSIFICATION OF THIS PAGE (When Data Entered)

Table of Contents

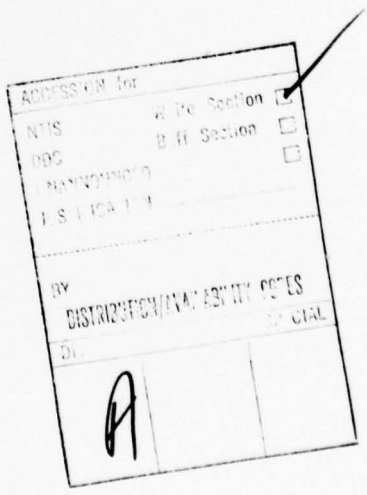

List of Illustrations

1. INTRODUCTION

The research described in this report, as was the case in the previous interim report [1] (AFOSR-TR-76-0841, May 1976), is generally concerned with the analysis of stress in the vicinity of cooling holes in a gas turbine engine blade with transpiration or film cooling[1]. A schematic diagram of a typical blade is shown in Figure 1. As previously described, when such a blade is in service, the blade material is subjected to a thermomechanical stress environment. Of particular interest for purposes of the ongoing research is the "vicinity" of a single cooling hole, Figure 2, where the thermomechanical stress concentrations of interest are likely to occur.

2. BRIEF SUMMARY OF RESEARCH THROUGH 30 APRIL, 1976

As was reported in [1], two basic computer programs were created, based on the Boundary Integral Equation (BIE) method of numerical analysis for thermo-mechanical problems.

The first program, now designated L3CV, is a steady-state heat-transfer-analysis program capable of providing, numerically, those values of temperature θ and normalized heat flux θ_n on the surface of a body which are not initially prescribed as part of a well posed heat transfer problem. Specifically, the formula which forms the basis of this program may be written

$$\left[\underset{\sim}{E} \right] \left\{ \underset{\sim}{\theta} \right\} = \left[\underset{\sim}{G} \right] \left\{ \theta_n \right\} \qquad (1)$$

where $\underset{\sim}{\theta}$ and $\underset{\sim}{\theta}_n$ are discrete values of temperature and normalized flux at

---

[1] Specific blade configurations and data supplied by General Electric, Evendale, Ohio.

selected nodal points on the body surface and $\underset{\sim}{E}$ and $\underset{\sim}{G}$ are square matrices derived from the integrals of the kernel functions and shape functions over a surface pattern of elements. The basic ideas surrounding formula (1) are given in some detail in [1].

The second program, now designated TE3D, is a thermomechanical stress analysis program capable of providing, in its basic form, numerical values of thermoelastic surface traction $\underset{\sim}{t}$ from input data for a well posed thermoelastic problem. Specifically, the formula which forms the basis of this program may be written[2]

$$\left[\underset{\sim}{A}\right]\left\{\underset{\sim}{u}\right\} - \left[\underset{\sim}{B}\right]\left\{\underset{\sim}{t}\right\} = \left[\underset{\sim}{C}\right]\left\{\underset{\sim}{\theta}\right\} - \left[\underset{\sim}{D}\right]\left\{\underset{\sim}{\theta}_n\right\} \tag{2}$$

in which $\underset{\sim}{u}$ is a column of discrete surface displacement components, $\underset{\sim}{\theta}$ and $\underset{\sim}{\theta}_n$ are the same as in (1), and the matrices $\underset{\sim}{A}$, $\underset{\sim}{B}$, $\underset{\sim}{C}$, $\underset{\sim}{D}$ are derived from kernel and shape functions as are $\underset{\sim}{E}$ and $\underset{\sim}{G}$. Again, detail surrounding formulas (1) and (2) is found in [1].

As employed for purposes of report [1], and as described therein, formulas (1) and (2) were subject to a number of limitations in generality and efficiency, which to a large degree have been removed. Details concerning such improvements are described in the present report.

The problems, described in [1], upon which programs L3CV and TE3D were brought to bear were, it will be noted, largely of the "test" variety, i.e. problems with varying degrees of similarity to the research problem but sufficiently idealized to check our programs by comparison of results with

---

[2] Zero mechanical body force is assumed in (2).

accepted solutions. Although at this writing the "research problem", as described in [1] and as more fully discussed subsequently, has not yet been fully solved, important steps toward this end have been taken as will be apparent. All of this research, as previously and presently reported, is directed toward a detailed investigation of the state of thermal stress in the vicinity of a single cooling hole in the turbine blade (cf. Figs. 1,2,5). Our specific progress since 30 April 1976 follows.

3. PROGRAM IMPROVEMENT FEATURES

3.1 MORE GENERAL BOUNDARY CONDITIONS

As actually used in [1] for the reasons stated therein, the computer programs to implement formulas (1) and (2) were written to accept only $\underset{\sim}{\theta}$ as input data for heat transfer problems, and non-zero $\underset{\sim}{t}$ as input only on so-called "top" surfaces of the test problems.

Presently the heat transfer program L3CV will accept not only an appropriate description of $\underset{\sim}{\theta}$ or $\underset{\sim}{\theta}_n$ at relevant places on the surface of a heat conducting body, but also will accept a convective boundary condition of the form

$$\theta_n = h_c(\theta_o - \theta) \tag{3}$$

in which h and θ_o are known functions. This improvement in flexibility of acceptable boundary conditions is not only an intrinsic improvement in the program, but has made possible the acceptance of the same h and θ_o used by General Electric to calculate the temperature field in the vicinity of a cooling hole via their finite element scheme. A description of our heat transfer study based on General Electric data is given in Section 4.2 of the present report.

As an additional improvement the thermoelastic program TE3D will now accept non-zero $\underset{\sim}{t}$ on all surfaces of an essentially prismatic body so that bending and twisting or other more general loading effects may be imposed on a body and not just simple "tension" as in the earlier versions of the program. Moreover, a built-in symmetry feature has been incorporated which permits, in a problem with "half" symmetry, the surfaces coincident with the plane of symmetry to not be discretized. This feature, although not always desirable to use even when possible (for reasons to be mentioned in Section 3.5), permits the use of a fewer number of nodes, with attendant saving in computer cost and other analysis effort. A "quarter" symmetry feature, allowing additional saving in this regard is currently being built into the program.

3.2 NEW QUADRATURE RULE FOR TRIANGULAR ELEMENTS

Upon mapping a curvilinear triangular element to a plane equilateral triangle, which is a basic process in the formation of matrices $\underset{\sim}{A}$, $\underset{\sim}{B}$, etc. recall that we were faced with the task of performing an integration over the plane triangle to obtain a number I_T in the form

$$I_T = \int_{\Delta} F(P_\eta, \xi) da_\xi . \tag{4}$$

where $P_\eta \notin \Delta$ and where $F(P_\eta, \xi)$ is the product of a shape function, kernel function, and the Jacobian of the mapping (cf. [1] Eq. 13 and Figs. 3, 4). To accomplish the integration in a symmetric fashion, the triangle was subdivided into three parts, over each of which a product Gaussian integration rule was used. However, the scheme used was somewhat artificial as applied to a triangular domain and was inefficient in terms of the total number of

integration prints used, since an unnecessarily high minimum number of prints was required over each of the three subdivisions.

As an alternative, we implemented a much more efficient and somewhat more analytically rigorous formula, given by Lyness [2], for quadrature over a triangle. Lyness' quadrature rule is exact for polynomials of given degree of not necessarily product form defined on an arbitrary plane triangle. Despite the fact that our integrands $F(P_\eta,\xi)$ are not polynomial forms in ξ, the Lyness scheme provided a noteworthy measure of improvement in our basic computational scheme as regards accuracy vs computer time in both basic programs.

3.3. THE ELEMENT SUBDIVISION QUESTION

The issue of subdividing an element into subelements before integrating, as referred to above and discussed in some detail throughout [1], was examined at some length in the course of the present research. Despite the seemingly heavy emphasis on this matter by Lachat and Watson [3,4], we found it to be relatively unnecessary to the success and basic efficiency of our integration schemes, and steps were taken to remove previously implemented subdividing processes. In addition to the case mentioned above with the triangles for $P_\eta \notin \Delta$, we removed the circular subdivisions (cf. [1] Fig. 5) for the $P_\eta \in \Delta$ or $\square$ case with no loss in accuracy and some gain in efficiency. A private communication from Lachat and Watson indicated an overemphasis on the subdivision issue in their work in retrospect. The process was used less in actual fact than reading their papers would indicate and is an issue subject to reexamination from their point of view.

3.4 SELECTIVITY IN DEGREE OF INTEGRATION

Lachat and Watson [3,4] describe criteria for subdividing an element before

integrating and for selection of the number of integration points to use to obtain a sufficiently accurate value for a required integral, e.g. (4). This process (cf. [3] pg. 104 et. seq.) is based primarily on the behavior of the kernel function and ignores completely the variation in the Jacobian function. In our experience, most if not all of the kernel function variation, assuming constant Jacobian, could be handled well with a threshold number of integration points, whereas the variation in the Jacobian is the item most requiring the selectivity process. More specifically, since in our programs all quadrilateral elements are mapped to a square and all curvilinear "three-sided" elements are mapped to an equilateral triangle, the variation in Jacobian is directly related to the distortion or departure of a given element from the mapped shapes. Thus, we have implemented a process whereby we choose the "degree of integration" for a given segment, i.e. "how many integration points to use" on the basis of distortion of the element. Presently this process is an observational one and we are taking steps to automate it. Nevertheless, this process has been responsible for some measure of accuracy vs running time efficiency in our programs and often allows us to "get by" with a cruder surface discretization and hence a smaller number of nodes (and consequently reduced overall problem size) for a given thermo-mechanical stress analysis problem. This matter is discussed further subsequently.

3.5 BOUNDARY AND INTERNAL STRESS CALCULATIONS

As indicated in the discussion of formula (2), the thermoelastic traction $\underset{\sim}{t}$ is usually, and has been, the output of greatest interest in test problems thus far. Specifically, problems have been modelled with surface nodes placed in such a manner that the t_3 component of $\underset{\sim}{t}$ has been identical

with the peak normal stress σ_{33} of greatest interest. Nevertheless, if the built-in symmetry feature is used and/or if other components of boundary stress not identical with the components of $\underset{\sim}{t}$ are desired, it is possible to obtain such boundary stress components according to the following scheme.

At the surface of a body the traction components t_i are related to the stress components σ_{ij} and components of the unit normal n_j according to

$$t_i = \sigma_{ij} n_j \tag{5}$$

Further, Hooke's Law,

$$\sigma_{jk} = \frac{2\mu\nu}{1-2\nu} u_{m,m}\, \delta_{jk} + \mu[u_{j,k} + u_{k,j}] - \delta_{jk}\gamma\theta \tag{6}$$

relates the surface stresses to the components $u_{i,j}$ of displacement gradient and the temperature. Now, since these same displacement gradient components are related to in-plane derivatives $u_{i,\xi\rho}$ of u_i according to

$$u_{i,\xi\rho} = u_{i,j}\, x_{j,\xi\rho} \qquad \rho = 1,2 \tag{7}$$

it is possible to solve (5), (6), and (7) simultaneously for the desired components of surface stress and, incidentally, the surface displacement gradient components, if desired.

As is apparent, the traction components t_i and in-plane derivatives $u_{i,\xi\rho}$, along with the coordinate gradients $x_{j,\xi\rho}$, normal components n_i and elastic constants are required as input. In-plane gradients are input in terms of nodal values of u_i and x_i with the aid of the shape function representations

$$\begin{aligned} u_i(\xi) &= M^{\alpha}(\xi)\, u_i^{\alpha} \\ x_i(\xi) &= M^{\alpha}(\xi)\, x_i^{\alpha} \end{aligned} \tag{8}$$

The boundary stress field obtained as described above depends most, for accuracy, on the accuracy with which the $u_{i,\xi\rho}$ and $x_{j,\xi\rho}$ are given by (8). Results using this process are largely satisfactory with, perhaps, the $u_{i,\xi\rho}$ being of lesser accuracy than $x_{j,\xi\rho}$ in any given problem. Nevertheless, we generally expect the t_i components themselves to be of greater accuracy than any of the boundary σ_{ij} obtained from them as described above. Thus, whenever the t_i components can be made identical with the boundary σ_{ij} of greatest interest, equations (5) through (7) need not be used and this is often the recommended procedure. However, the boundary stress process above is required, as is the internal stress procedure to follow, whenever the built in symmetry feature is used, or, of course, when components of σ_{ij} not identical with t_i are required.

Regarding the internal stress field σ_{ij} which may be desired at an arbitrary *volume point p, consider first the internal* displacement field u_i, which, under the discretization assumptions described fully in [1] and zero body force, takes the form

$$u_j(p) = t_i^{\alpha\sigma} \int_{S_\sigma} M^\alpha(\xi) U_{ij}(p,Q(\xi)) J(\xi) d\xi - u_i^{\alpha\sigma} \int_{S_\sigma} M^\alpha(\xi) T_{ij}(p,Q(\xi)) J(\xi) d\xi$$

$$+ \mu_o \gamma \theta^{\alpha\sigma} \int_{S_\sigma} M^\alpha(\xi) \frac{\partial r,_j}{\partial n}(p,Q(\xi)) J(\xi) d\xi - \mu_o \gamma \left(\frac{\partial \theta}{\partial n}\right)^{\alpha\sigma} \int_{S_\sigma} M^\alpha(\xi) r,_j(p,Q(\xi)) J(\xi) d\xi$$

$$+ \mu_o k_o \sum_{\sigma=1}^{m} \int_{S_\sigma} n_i(Q(\xi)) r(p,Q(\xi)) J(\xi) d\xi \qquad (9)$$

where $\theta,_{ii} = k_o$. Notation and definition of variables in (9) is exactly the same as that for equations (1) through (8) in [1], and it is important to note that all quantities to the right of the equal sign are known following

the solution of the boundary integral equation (2). Should $u_j(p)$ be desired, it suffices to evaluate the above integrals and perform the indicated summations upon specifying the coordinates of p. Further, p being an interior point, all evaluation of the integrals (cf. Eq. (11) in (1) and Eq. (4) of the present report) are in the $p \notin S_\sigma$ category and thus, although requiring careful attention, they are non-singular.

With formula (9) in hand, the internal stress field σ_{jk} is related to the displacement gradient field $u_{j,k}$ according to Hooke's Law (6) referred to the interior so that gradients of $u_j(p)$ via equation (9) are required. Explicitly, since only the kernel functions under the integrals in (9) are functions of p, the appropriate expression for the gradient field $u_{j,k}(p)$ is identical with (9) with U_{ij}, T_{ij}, $\partial r,_j/\partial n$, $r,_j$, and r replaced respectively by $U_{ij,k}$, $T_{ij,k}$, $\partial r,_{jk}/\partial n$ and $r,_k$. Subsequent insertion into equation (6) in a straightforward manner yields the appropriate interior stress field directly. Again, of course, the integrals are non-singular.

4. SOLVED PROBLEMS

4.1 ANOTHER TEST THERMAL STRESS PROBLEM

In section 4.5 of [1], an elementary test thermoelastic problem was briefly mentioned as a check on our program's capability to incorporate satisfactorily the two terms on the right side of Equation (2). No data were reported for this problem in [1]. Subsequently we have used a finer discretization to obtain a more accurate solution. A detailed description of the problem and results follows.

Consider a hollow cylinder with inner and outer radii, a, b, respectively, and height h. We subject the cylinder to the steady-state temperature $\theta(\rho) = C_1 + C_2 \ell n\, \rho$, $a \leq \rho \leq b$, where C_1 and C_2 are conveniently chosen

constants, i.e., $C_1 = 1$, $C_2 = -1/\ell n(0.4)$. The top and bottom surfaces of the cylinder are held against normal displacement, while the lateral surfaces. though not traction free, are subject to zero net force and moment. (See [5] pg. 290 for specific traction distribution and associated analytical thermoelastic stress field with which we compare results). We model one quarter of the cylinder as shown in Fig. (3), with $m = 24$ segments and $n = 74$ nodes. Using $a = 0.4$, $b = 1.0$, $h = 1.0$ with convenient values for all other relevant parameters, numerical results for values of thermal stress and displacement compared with expected analytical results are as reported in Table I.

Using the same geometrical and material parameters and discretization pattern, we now subject the cylinder to the temperature distribution[3] $\theta(z) = (1/h^2)[h^2 - z^2 + hz]$, $\sigma \leq z \leq h$. Here the top and bottom surfaces of the cylinder are traction free and hence free to warp. The lateral surfaces, while again not traction free, are subjected to a specified traction distribution (see Reference [5], pg. 278) with zero net force and moment. Results for relevant values of thermal stress and displacement are as reported in Table II. For each of the above problems we used "degree 3" integration for all segments (see discussion in Sections 3.4 and 4.3) and the CPU times on an IBM 370, model 165, (et. seq. for all subsequent computations) are 2 min. 31 sec. and 2 min. 52 sec., respectively.

---

[3] Note $\nabla^2\theta = -2\theta_0/h^2 \neq 0$ here, but since $\nabla^2\theta$ = constant, equation (2) is still valid with the simple addition of another known term, cf. [6], Eqs. (7) and (10).

Table I Results for Thermoelastic Cylinder with Radial Temperature Variation

Coordinate ρ	Radial Displacement BIE	Radial Displacement Exact	Transverse Stress BIE	Transverse Stress Exact	Axial Stress BIE	Axial Stress Exact
0.40	0.325	0.322,	0.837	0.857	0.198	0.215
0.55	0.347	0.346	0.262	0.254	-0.237	-0.248
0.70	0.454	0.453	-0.088	-0.082	-0.610	-0.599
0.85	0.615	0.611	-0.302	-0.307	-0.884	-0.882
1.00	0.807	0.806	-0.473	-0.474	-1.116	-1.118

Table II Results for Thermoelastic Cylinder with Axial Temperature Variation

Coordinates z	Coordinates ρ	Radial Displacement BIE	Radial Displacement Exact	Axial Displacement BIE	Axial Displacement Exact	Transverse Stress BIE	Transverse Stress Exact
0	0.40	0.266	0.267	-0.081	-0.080	-0.459	-0.444
	0.70	0.468	0.467	-0.246	-0.245	-0.452	|
	1.00	0.670	0.667	-0.500	-0.500	-0.439	|
0.25	0.40	0.368	0.367	0.247	0.248	-0.356	-0.361
	0.70	0.643	0.642	0.082	0.083	-0.349	|
	1.00	0.917	0.917	-0.173	-0.172	-0.346	|
0.50	0.40	0.467	0.467	0.586	0.587	-0.124	-0.111
	0.70	0.818	0.817	0.420	0.422	-0.119	|
	1.00	1.170	1.167	0.164	0.167	-0.103	|
0.75	0.40	0.569	0.567	0.882	0.884	0.319	0.305
	0.70	0.993	0.992	0.717	0.719	0.319	|
	1.00	1.418	1.417	0.460	0.464	0.319	|
1.00	0.40	0.667	0.667	1.084	1.087	0.883	0.889
	0.70	1.170	1.167	0.920	0.922	0.883	|
	1.00	1.672	1.667	0.661	0.667	0.891	|

4.2 HEAT TRANSFER ANALYSIS FOR THE RESEARCH PROBLEM

With the program improvement features described above and the general increased level of confidence in our computer programs, we attempted a heat transfer analysis of the "research problem" as depicted in Figure 2 and somewhat more to scale in Figure 4. From General Electric we obtained the necessary geometrical, mechanical, and thermal material data for the body of Figure 4, along with data for h_c and θ_o in the boundary condition Equation 3. More specifically, numerical values of the film coefficient h_c and the adiabatic wall temperature θ_o were provided, more crudely than we would have liked, but nevertheless in sufficient detail to describe proper boundary conditions over the surface element pattern of Figure 4. After some experimentation we used a total of 48 surface elements and 142 nodes. Via program L3CV (re. Eq. (1)) we calculated (67 sec. CPU time) surface values of temperature $\underset{\sim}{\theta}$.

Agreement with corresponding values of $\underset{\sim}{\theta}$ as provided by General Electric via a finite element analysis was generally satisfactory although checking the integrity of our calculated surface values of $\underset{\sim}{\theta}$ by direct detailed comparison point by point with those values of $\underset{\sim}{\theta}$ accepted by General Electric is difficult for the following reasons. Their heat transfer analysis was a finite element analysis of essentially a whole cross-section of the blade of interest, where temperatures associated with the elements in Figure 5, assumed constant over the elements, are obtained. Our BIE solution for the body of Figure 4 (cf. shaded region Fig. 5) is based on a somewhat finer surface grid, although no finer than that justified on the basis of the somewhat crude h_c and θ_o input information mentioned earlier. Moreover, we considered temperature to vary quadratically over each element. Thus, since our temperatures are obtained at our surface element nodes, we have a finer picture of

the temperature distribution in the region of interest. Nevertheless, our solution is basically consistent with the General Electric solution, showing temperatures of comparable magnitude (approximately 1700-1800°F) with expected hotter and cooler areas in the proper locations although their solution is a bit cooler than ours (by 170° or so) in the upstream vicinity of the cooling hole. One reason for this difference is that we chose to ignore the effect of a "junction" hole (between the two left-most circular cooling chambers of Figure 5) which, according to a recent communication with heat-transfer personnel at General Electric, would have an additional cooling effect and could easily account for some of the differences. Nevertheless, as this report is being written, we are obtaining from General Electric a better description of h_c and θ_o over the surface than was initially used. This is not so much for purposes of the heat transfer analysis itself, but for input into TE3D for the same body (Sec. 5.2) and for input into our proposed parameter studies (Sec. 5.3).

An additional check on the reliability of our heat-transfer analysis described above was made prior to that analysis and is described in the following. A block of material of identical shape and properties as the body of Figure 4, but without the cooling hole (lower curved surface of Fig. 4), was imagined imbedded in a thick plate in a state of one-dimensional heat flux. Values of h_c and θ_o for use in Equation (3) for the test temperature field could thus be calculated analytically and then put on as boundary conditions for the mentioned block of material. Surface temperature data were then obtained from program L3CV and compared with analytical temperature data. This was carried out using the same discretization described above. Agreement was excellent everywhere, as expected. This little exercise provided a meaningful test of the workings of L3CV insofar as its ability to handle the types

of boundary conditions and the basic body shape needed above. It also provided some measure of the basic adequacy of our discretization for this type of problem, keeping in mind, of course, the absence of the cooling hole.

4.3 ISOTHERMAL ANALYSIS OF PLATE WITH SKEW HOLE

One big issue, perhaps the biggest, to face in the stress analysis of the "research problem" is the skewness of the cooling hole; specifically, the angle of the axis of the hole is 60° with the "front" surface normal (cf. Figs. 2 and 4). In our previous experience with stress concentrations induced by holes (e.g. [1] Secs. 4.3, 4.4), we put off the skewness issue which now we must face.

Ellyin [7,8] has conducted a series of experiments to determine the stress concentration in the vicinity of such skew holes in flat plates. Appropriate analytical results seem to be unavailable for understandable reasons. Thus, we decided, as a meaningful and prudent prelude to the "research problem", to attempt a BIE analysis of a portion of an "Ellyin type" plate and compare results.

In Figure 6 is shown one symmetric half of a plate with a 60° skew hole loaded in tension at the top with a uniform normal traction σ_0. The boundary condition at the bottom of the plate is zero normal displacement and zero shear traction as is dictated by symmetry. The unknown normal traction on the bottom therefore is coincident with the component of stress of most interest. The rest of the surfaces of the plate are assumed traction free. Width, thickness, and hole diameter dimensions and material properties are chosen as in [8]. Note, except for the width and thickness dimensions and, of course, the flatness of the "back side" of the Ellyin plate compared to the irregularity of the "back side" of the research problem body Fig. 4, there is essential similarity of geometry in the vicinity of the skew hole.

Ellyin [8] predicts a stress concentration σ_{max}/σ_o at or near[4] the feather edge of the hole of slightly more than 8. Our first attempts to reproduce this value based on the somewhat crude discretization pattern of Figure 7 with m = 53 segments, n = 122 nodes were high of the mark. Three computer runs were made with three levels of sophistication in the "degree of integration" as discussed in Section 3.4.

The first and crudest run yielded a highly fictitious stress concentration $\sigma_{max}/\sigma_o = 31.4$ in 163 sec. CPU time. This "degree 1" run involves a minimum, threshold number of integration points (4 for rectangular segments, 6 for triangular segments) in all integrations. The second run yielded $\sigma_{max}/\sigma_o = 15.1$ in 337 sec. CPU time, where we were selective in the degree of integration, from "degree 3" for certain integrations, "degree 2" for others, and "degree 1" for the remaining integrations. Degree 2 involves 9 integration points for rectangles and 7 integration points for triangles, whereas degree 3 requires 16 integration points for both rectangles and triangles. Selectivity was based primarily on the distortion of the element as discussed in Section 3.4 but also to some extent on the proximity of the element to the region of interest. As mentioned in Sec. 3.4, we are still experimenting with this selectivity feature. A third run using degree 3 for all integrations yielded $\sigma_{max}/\sigma_o = 12$ in 579 sec. CPU time, which is closer to the expected value of 8, but still unacceptable, of course.

Clearly, our discretization of Figure 7 is too crude to obtain an acceptable stress analysis for this problem. However, rediscretizing, i.e. adding more segments and nodes to the full half-plate would have required more nodes

[4] The magnitude and precise location will be discussed further subsequently.

than we cared to deal with. Thus, we considered the consequences of cutting the half-plate in half, normal to the top surface and along the axis of the hole, yielding the "quarter-plate" shown in Figure 8. The problem of a suitable boundary condition on the new cut surface was resolved in favor of assuming zero in-plane shear traction and normal displacement of zero. We believe that whatever departure from this boundary condition is present in the full plate would have a minimum effect on the stress concentration of interest.

Our renewed attempt on the problem using the quarter-plate of Figure 8 involved $m = 54$ segments and $n = 136$ nodes. Not only is the discretization, shown in Figure 9, much finer with fewer distorted elements, and thus more appropriate to the task, but the height of the quarter-plate (at the top of which the load σ_o is applied) was made greater to better agree with the height dimension chosen by Ellyin [8], who also was trying to simulate uniform tension at infinity. Our first "degree 1 everywhere" computer run (CPU 221 sec., called Run a) revealed the dramatic improvement associated with the mentioned changes. A second "selective degree" run (CPU 406 sec., called Run b) using degree 1 on most segments away from the hole, degree 2 on nearer segments, and degree 3 on all non-plane segments (i.e. those on the hole) and those nearest the feather edge produced our best results. Results from both runs are shown in Figure 10.

In Figure 10 is plotted the variation of normal stress along the edge of the hole (line AB of Fig. 7) as predicted by the two runs described immediately above, along with Ellyin's [8] experimental data. In Figure 11 is shown the variation of normal stress along line AC (of Fig. 7) of the plate. (Ellyin has no corresponding results for comparison.)

We regard our results, especially Run b of Figure 10, as an acceptable solution to this skew-hole problem. All obvious features of the solution such as smoothness of the data shown (as well as that not shown), balance of equilibrium, and of course closeness to Ellyin's [8] believable results are better than in any of our previous runs. Moreover, our experience with similar (albeit less demanding) problems would indicate that any further refinement in surface element resolution and/or degree of integration would yield negligible further improvement in results. This would be done, we might add, only at considerable effort and expense.

Regarding the all-important level and distribution of stress along the edge of the hole as shown in Figure 10, Ellyin [7] has a number of plots, similar to Figure 10, where the angle of inclination of the hole with the plate normal varies from 0° to 45° in 15° increments. (Our treatment of the 0° case is discussed in [1], Sec. 4.4.) He shows that the location of the stress concentration moves nearer to the surface of the plate (i.e. point A) as the angle of inclination increases. However, he suggests that in each case the level of stress right at the surface of the plate is lower than the peak value some distance in from the surface. The precise location of the peak value, as Ellyin [7] discusses, is subject to some uncertainty, and how close to the surface its precise location is for a 60° hole is not at all clear in [8]. Nevertheless, on theoretical grounds, a smooth progression from 0° to 60° or larger angles, with peak stress moving nearer the surface of the hole but having an ever smaller "tail" (as suggested in Fig. 10), is most believable. Our best data, Run b, suggests such a tail. In any case, the picture of "edge-of-the-hole" stress in Figure 10 according to our computations agrees sufficiently well with Ellyin [7,8] for us

to proceed with confidence to the next phase of the research problem. The above represents the most stringent test of our BIE analysis capability thus far, and we are pleased with the results. These results were communicated, at a conference on June 29, 1977, to the interested people at General Electric. They are, as are we, anticipating with great interest the thermal stress analysis results we are prepared to obtain.

5. RESEARCH IN VARIOUS STAGES OF COMPLETION

5.1 ISOTHERMAL ANALYSIS OF THE RESEARCH PROBLEM

Before beginning a description of the analysis of this problem the following comments are in order. Although it was possible to employ the built-in "half-symmetry" feature of our program in the skew hole analysis of section 4.3, we did not do so, in order to obtain the stress concentration directly in the form of tractions, as discussed in Section 3.5. Further, the saving in nodes and surface discretization would have been minimal due to the thinness of the plate. However, for the research problem body, (cf. Fig. 4), using the symmetry feature and thus not having to discretize the lower plane horizontal surface would clearly be most advantagous. There would be considerable saving in discretization effort as well as nodes. Even so, the total number of nodes needed promises to be considerable, i.e. upwards of $n = 160$. We are presently working on a discretization pattern, with a feasible number of nodes, that will be adequate not only for our isothermal analysis but also for our thermomechanical analysis.

Concurrent with this activity is calculation of the stress-patterns of Figure 10 via the boundary stress process of section 3.5 in order to compare with the data of Figure 10, obtained by direct traction output from TE3D as explained earlier. This more stringent test of our boundary stress capability

is necessary, as is additional checking of our interior stress capability, since we will rely exclusively on these capabilities (rather than direct tractions) to yield the stresses of interest when using the built-in symmetry feature for the research problem.

The boundary condition on the "top" surface of Figure 4 for the isothermal stress analysis is, more properly, a prescription of uniform normal displacement rather than uniform normal traction as was used on the plate of the previous section. This is dictated by the assumption of conditions of symmetry across "horizontal" planes between cooling holes (cf. Fig. 1). The two boundary conditions are not equivalent except in the limit as the distance between holes becomes arbitrarily large. Thus, it is of interest to note the difference in "stress concentration" between uniform traction and uniform normal displacement as the prescribed boundary condition on such a top surface a finite distance from the hole. We are in the process of investigating this difference, to assess its significance, in connection with the skew-hole problem of the plate of the previous section. We anticipate that the applied traction on the top of such a body corresponding to a uniform displacement is nonuniform in such a manner as to relieve the stress concentration from its former value. Thus we expect, on that ground alone, lower levels of isothermal stress concentration for the research problem. Further, the thickness of the body and the less-severe "feather" edge conditions at the upstream end of the hole should contribute further to lowering the stress concentration. If this is true, the analysis of the previous section is more demanding than for the research body, and the results predict a more conservative (higher) isothermal stress concentration. In any case, General Electric currently has no other basis for isothermal stress

concentrations for such skew holes and they conservatively use the higher value. The thermomechanical state of stress, however, is another story.

5.2. THERMOMECHANICAL ANALYSIS OF THE RESEARCH PROBLEM

The analysis to be outlined in this section is the focus of the entire investigation, insofar as the specific body configuration we have been working with is concerned. Since the body geometry and discretization are to be identical with those of the previous section, the basic issue here is that of thermal boundary conditions, i.e. we now have non-zero thermal input terms to TE3D for the research problem surfaces.

Specifically, surface temperature $\underset{\sim}{\theta}$ and flux $\underset{\sim}{\theta}_n$ as obtained and discussed in section 4.2 are presently available although we will make a preliminary L3CV run to fit the data to our new discretization.

Mechanical boundary conditions of zero traction on all surfaces except the "top" and "bottom" surfaces are reasonable statements although, as mentioned in [1], non-zero tractions are possible across "cut" (vertical) surfaces of Figure 2, i.e. surfaces which join the research problem body to the rest of the blade (junction of shaded with non-shaded solid portions of the blade in Fig. 5). The normal component of displacement will be taken as zero at the bottom and uniform at the top, while in-plane tractions are assumed zero on both top and bottom surfaces. These boundary conditions are sufficient input to TE3D, and the output of interest (with the aid of the stress programs of Sec. 3.5) will be the non-prescribed tractions and thermal stress on the top and bottom surfaces of the research body.

The outcome of this investigation, based on the above input to TE3D, will be the thermal stress distribution due to the nonuniform thermal field in the body. A thermal "stress concentration" concept is more difficult to

define than is the case with an isothermal problem. Nevertheless, a pattern of stress variation, with peak stresses, should emerge in the vicinity of the hole. An order of magnitude comparison for these stresses due to the thermal field with the stress-concentration of "8" discussed previously is of primary interest to us and to General Electric. Such information is at hand, pending the "tidying-up" operations described in section 5.1.

5.3 PARAMETRIC STUDIES

However much the analysis of the previous section may be the focus of this research project and however interesting the result, its outcome nevertheless provides information based on very specific geometrical, mechanical, and thermal data for a very specific blade configuration. It is therefore only sensible to ascertain the most important parameters of the input contributing to the thermal stress, vary these in a systematic fashion, and use the described analysis capability to provide information pertinent to a range of values of the important parameters. General Electric supports this view.

Specifically, we agreed that the geometrically-most-important feature of the cooling-hole configuration is the angle of the hole to the blade surface, and to a lesser extent the length of the hole is significant. Of least importance, we think, is the fairly complicated geometry at the upstream end of the hole ("backside of Fig. 4). Thus, an essential geometry to deal with for the parameter studies is the familiar plate-with-skew-hole, i.e. the geometry of section 4.3, Figure 6, and Figure 12.

Regarding the thermal boundary conditions, after a recent lengthy conference with the heat transfer personnel at General Electric, we decided on the following. A reasonable boundary condition on the back, or upstream side, of the plate is a constant h_c and constant coolant temperature in

Equation (3). The front, or downstream side, of the plate is more complicated in that the gas mixes with the coolant in zone A (shaded region, Figure 12). In the unshaded portion we again have constant h_c and θ_o, but in the shaded zone A, a variable h_c and θ_o are to be used over the region according to certain emperical relations currently under investigation. Source material for this investigation is forthcoming from General Electric with guidance to some extent by the studies in [9]. Also forthcoming is information to determine a suitable h_c and θ_o over the length of the cooling hole surface. Here, we understand, an emperical duct-flow equation involving these parameters is to be used with an entrance correction to give a more realistic set of values for h_c and θ_o on the hole surface near the unstream end. On the remaining surfaces, we may sensibly take a zero flux condition. With this basic setup, we regard the thermal patterns and consequent thermal stress to depend most upon variability of h_c from place to place on the surfaces and variability of the angle of inclination of the cooling hole. Further, these are the parameters most subject to change from hole to hole in a given blade and from one blade configuration to another. Thus, variation of these parameters will form the basis of our study.

The two basic steps in the analysis for a given set of parameters will be to i) solve via L3CV for the surface values of $\underset{\sim}{\theta}$ and $\underset{\sim}{\theta}_n$, and then ii) find via TE3D the thermal stress distribution with value and location of peak stress. Hopefully, information correlating the peak thermal stress as a function of the h_c distribution and hole inclination will emerge.

5.4 OTHER RESEARCH

Following the completion of the research in the previous three sections we hope to have provided General Electric with useful information regarding

the nature of stress in the vicinity of cooling holes in the film-cooled blades. Still in hand of course are the two programs which provide the analysis and which, we feel, remain quite valuable as tools for similar analyses.

Two major items in connection with the use of the programs require further investigation. Such investigation would contribute greatly to their ultimate efficiency. The first item is an optimization study regarding the degree of Gaussian integration to use as a function of i) shape of element to be integrated over, ii) proximity of the element to the region of interest, and iii) proximity of the point P_η to the element, for a given discretization. These items were discussed at some length earlier in the report. Basically, it will be recalled that choices of degree of integration presently are manually made on the basis of experience, primarily, and CPU time depends heavily on how often "high" degrees of integration are used. Further, fine, "regular" discretizations permit lower degrees of integration to be routinely used. However since such discretizations require increased problem size and consequent elevation of CPU time, the question of optimization with changes in discretization as a parameter also remains.

The second item, more straightforward, is the body-subdivision issue. Lachat and Watson [3,4] have shown that analysis efficiency, primarily in terms of reduced formation and solution time, can be introduced into computer programs of the present type by subdividing the body under investigation. This means that the body is imagined to be cut into two or more subbodies by means of imaginary surfaces on which are located additional nodes. Such surfaces, across which continuity of variables is maintained, introduce additional equations and unknowns into the system. However, if this process is implemented wisely (see criterion proposed [3,4]) not only is sparseness

introduced into the final matrix of coefficients, resulting in reduced solution time, but often fewer total non-zero coefficients need be calculated. This feature of body subdivisions becomes of greater importance as the size of the problem (size of n) necessarily increases. It can always be used with profit when surfaces across which gradients in variables are low are used for subdividing.

Both efficiency items are regarded as important, now that the programs have developed in sophistication sufficient to handle problems such as those described and even larger-scale problems. Investigation of these efficiency items are currently underway.

Finally, a program of research outlined in our most recent renewal research proposal (transmittal date March 1977) centers around modifications in our present capabilities and possible creation of new areas to include certain kinds of material anisotropy and possible inhomogeneity. This research is also underway.

REFERENCES

1. F. J. Rizzo and D. J. Shippy, "Thermomechanical Stress Analysis of Advanced Turbine Blade Cooling Configuration," AFOSR-TR-76-0841, May 1976.

2. J. N. Lyness, "Moderate Degree Symmetric Quadrature Rules for the Triangle," J. Inst. Maths. Applics. No. 15, 1975.

3. J. C. Lachat, "A Further Development of the Boundary Integral Technique for Elastostatics," dissertation University of Southampton, England, 1975.

4. J. C. Lachat and J. O. Watson, "Effective Numerical Treatment of Boundary Integral Equations: A Formulation for Three-Dimensional Elastostatics," Int. J. Num. Meth. Engng. No. 10, 1976.

5. B. A. Boley and J. H. Weiner, "Theory of Thermal Stresses," Wiley, New York, 1960.

6. F. J. Rizzo and D. J. Shippy, "An Advanced Boundary Integral Equation Method for Three-Dimensional Thermoelasticity," Int. J. Num. Meth. Engng. to appear.

7. F. Ellyin, "Experimental Study of Oblique Circular Cylindrical Apertures in Plates," Exp. Mech., Vol. 10, pp. 195-202, May 1970.

8. F. Ellyin and U.M. Izmiroglu, "Effect of Corner Shape on Elastic Stress and Strain Concentration in Plates with an Oblique Hole," Trans. ASME (J. Eng. Ind.), Vol. 95, p. 151-157, Feb. 1973.

9. S. Ito, R. J. Goldstein, and E.R.G. Eckert, "Film Cooling of a Gas Turbine Blade," Proc. 1977 Tokyo Joint Gas Turbine Congress, JSME and ASME Publication, May, 1977.

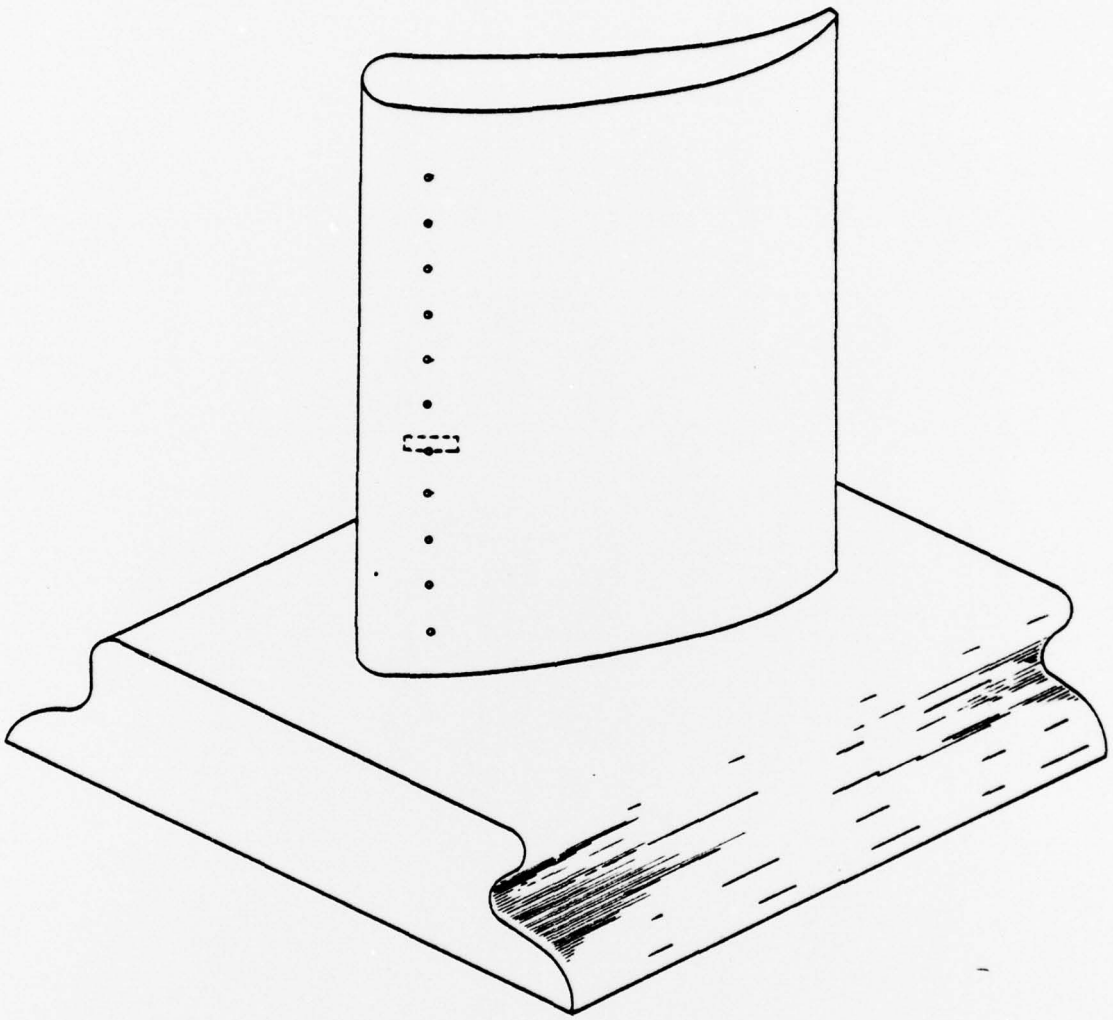

Figure 1. Schematic Diagram of Typical Turbine Blade

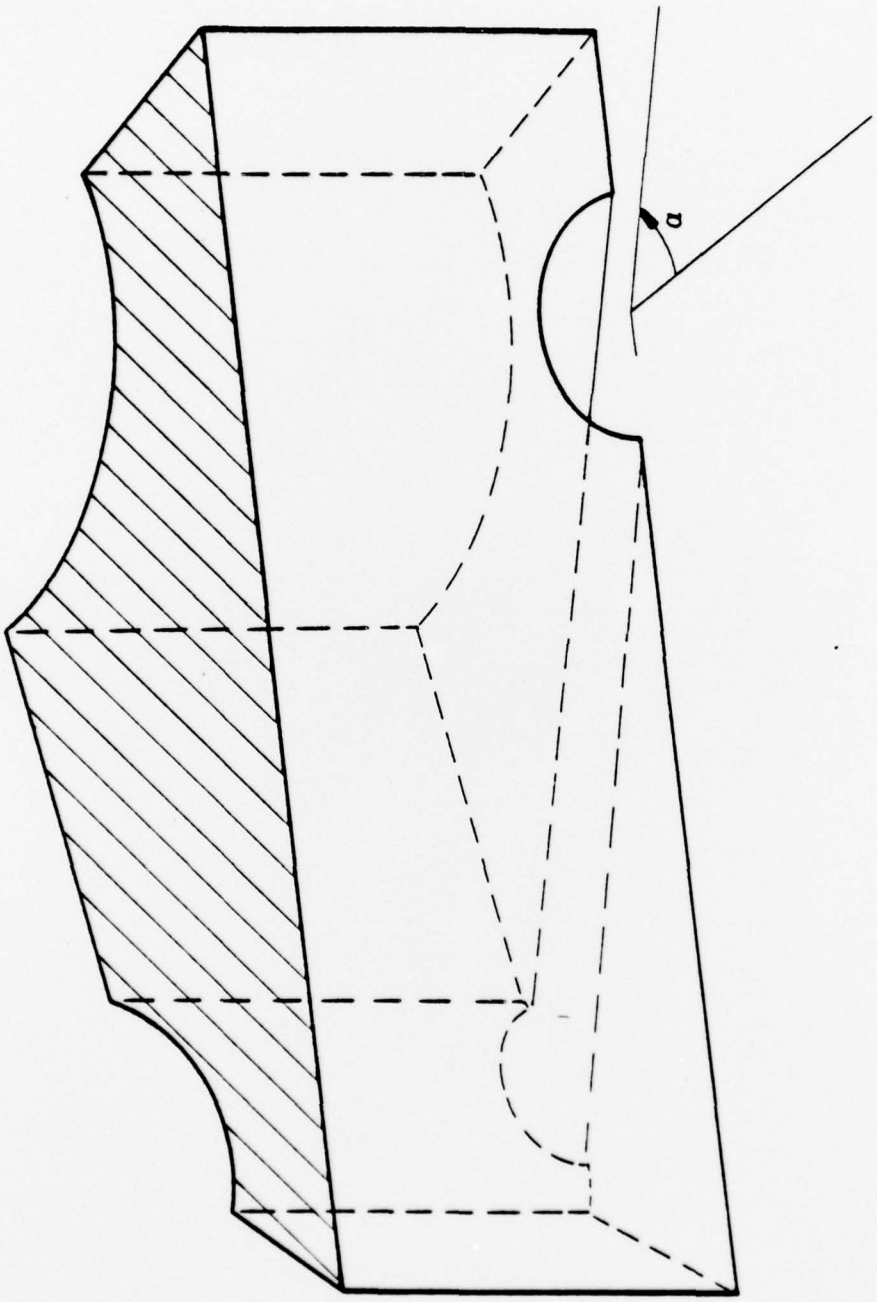

Figure 2. The Research Problem - "Vicinity" of Single Cooling Hole

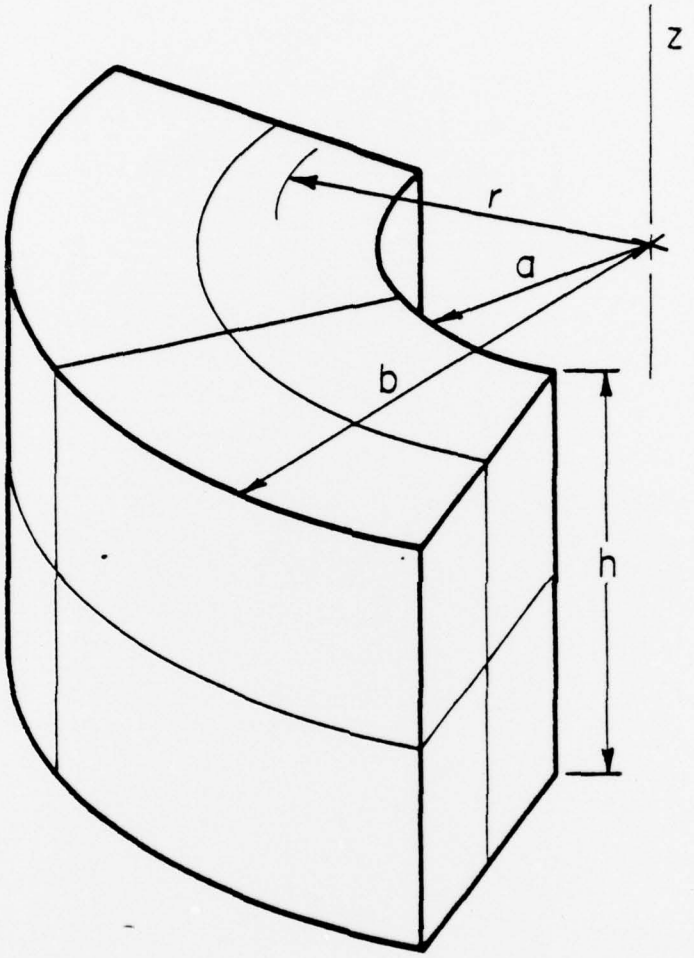

Figure 3. Quarter of Hollow Cylinder

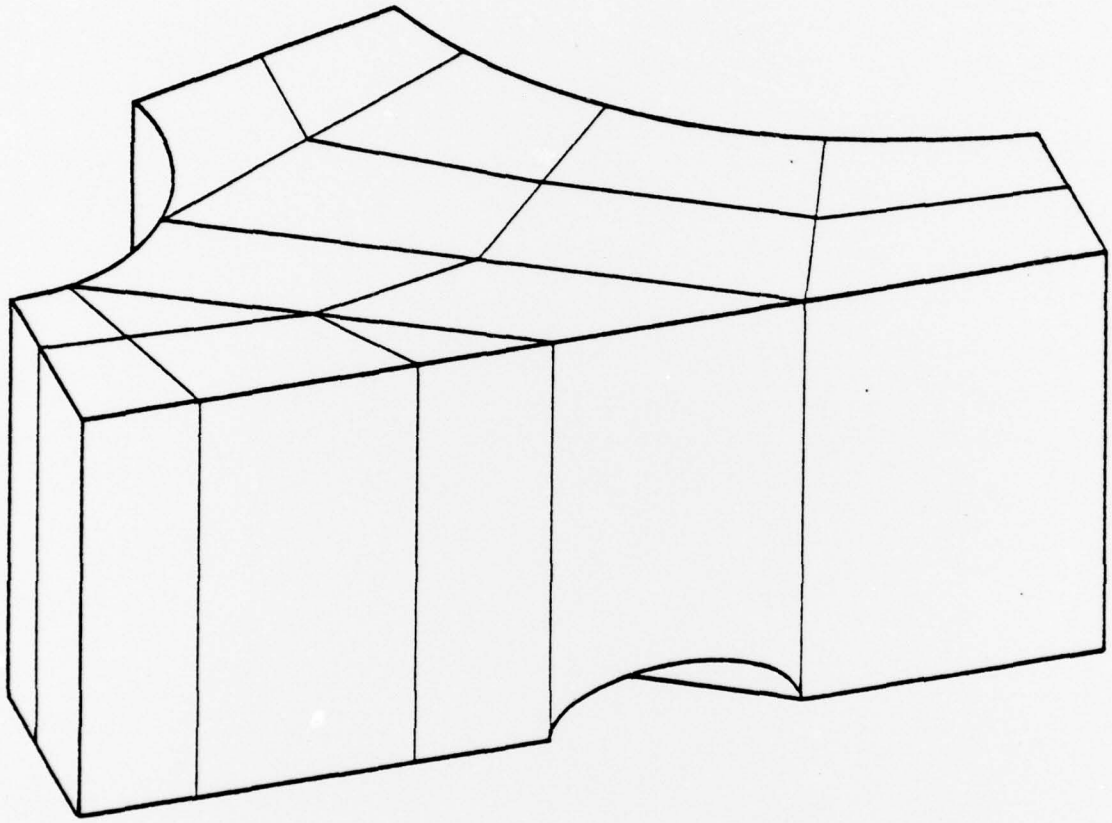

Figure 4. Surface Discretization of Research Problem

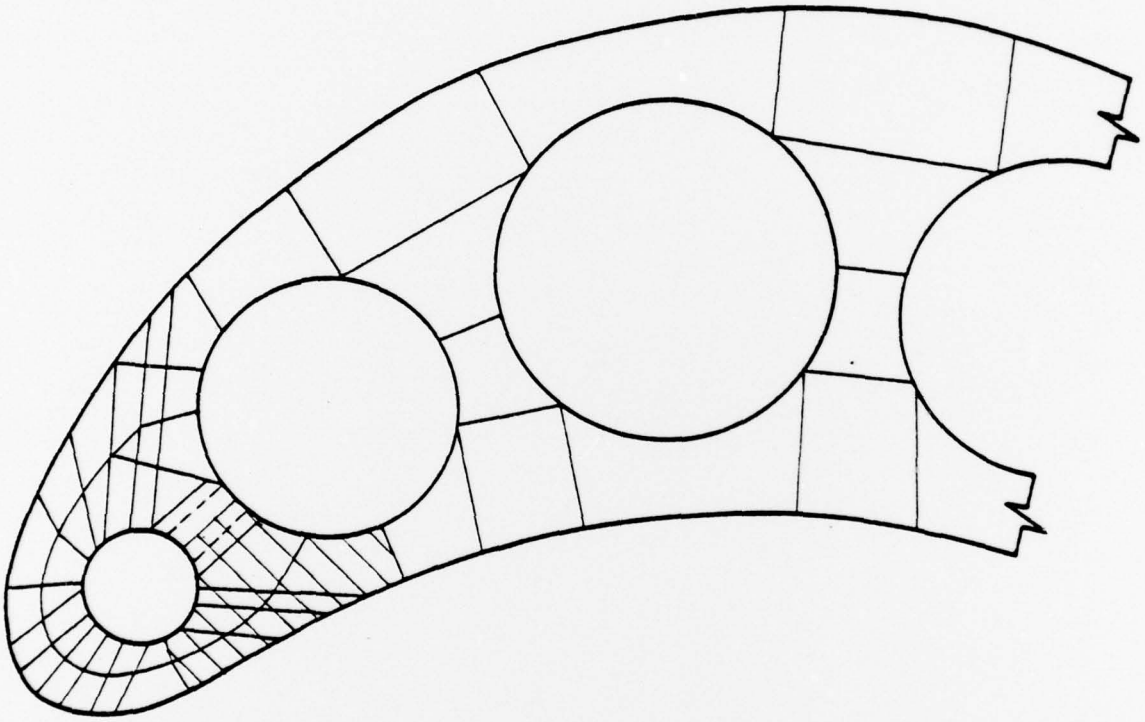

Figure 5. Cross-Section of Turbine Blade

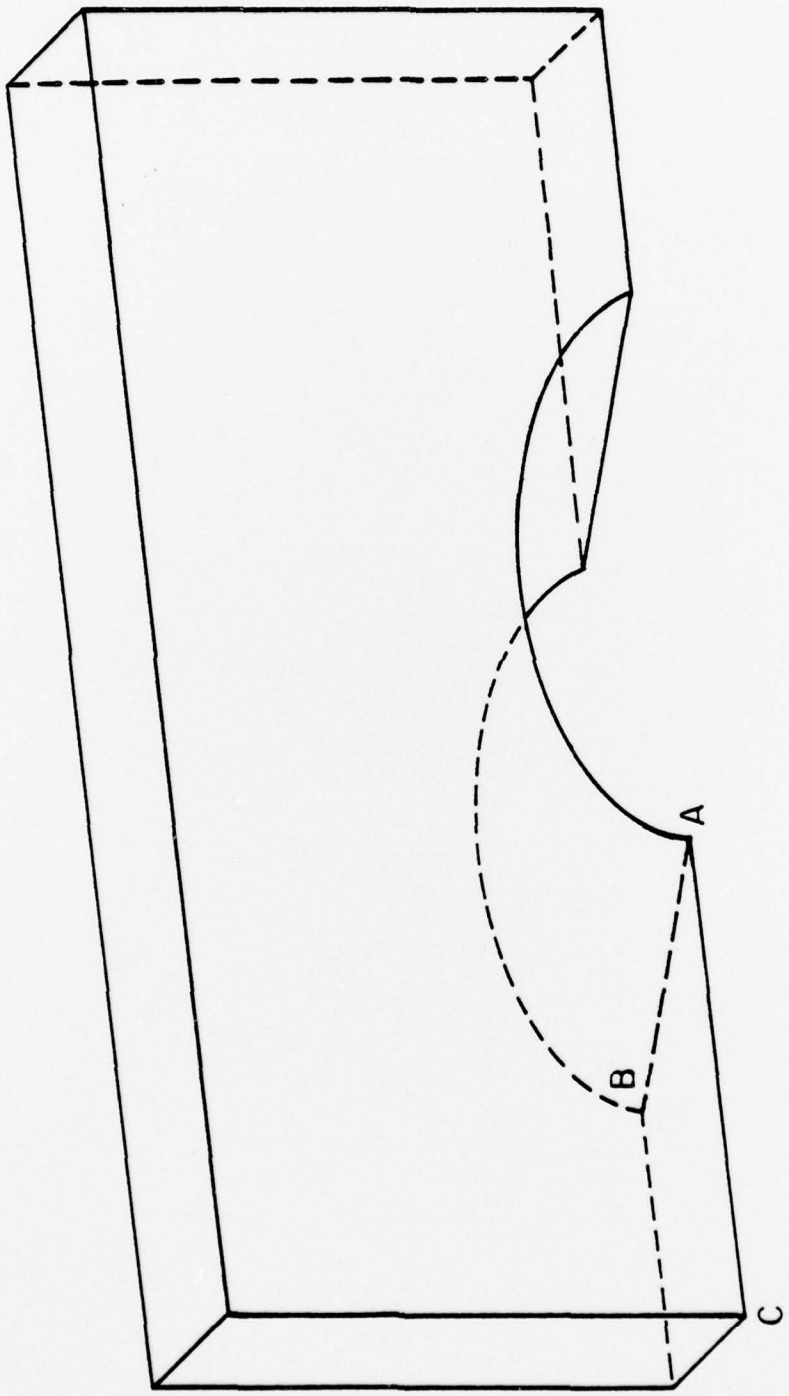

Figure 6. Half of Plate with 60° Skew Hole

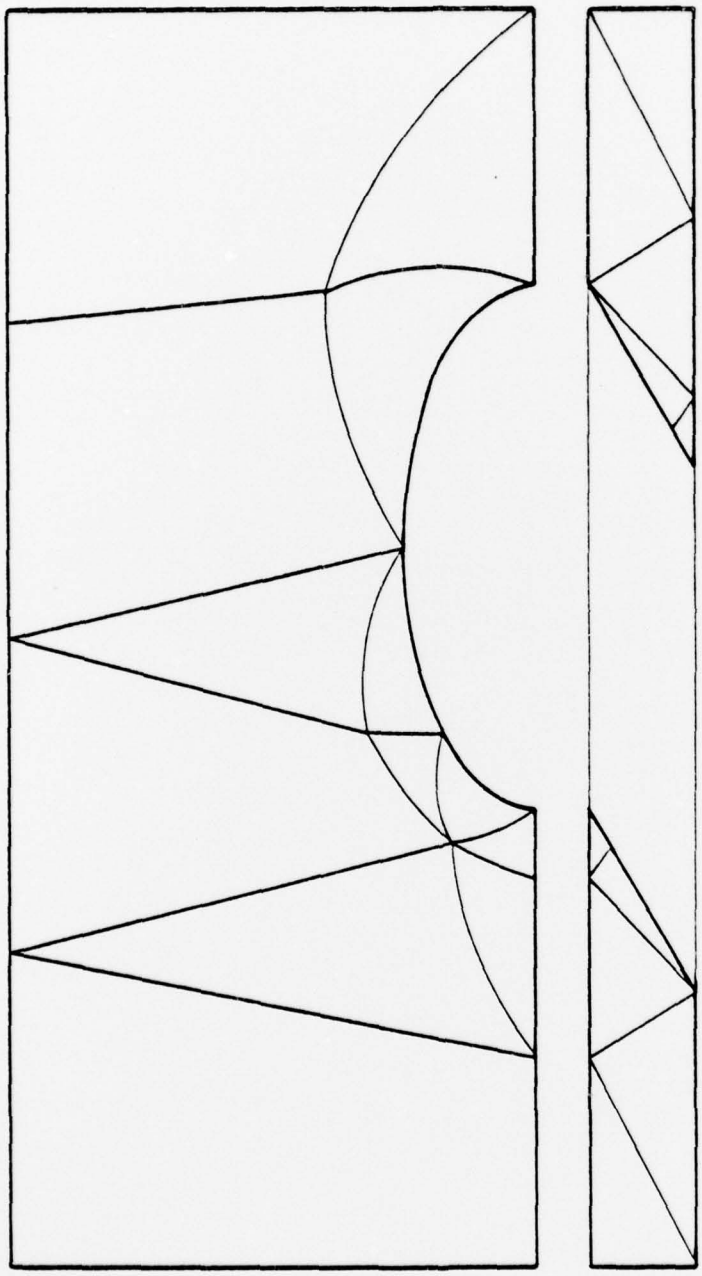

Figure 7. Surface Discretization of Half-Plate

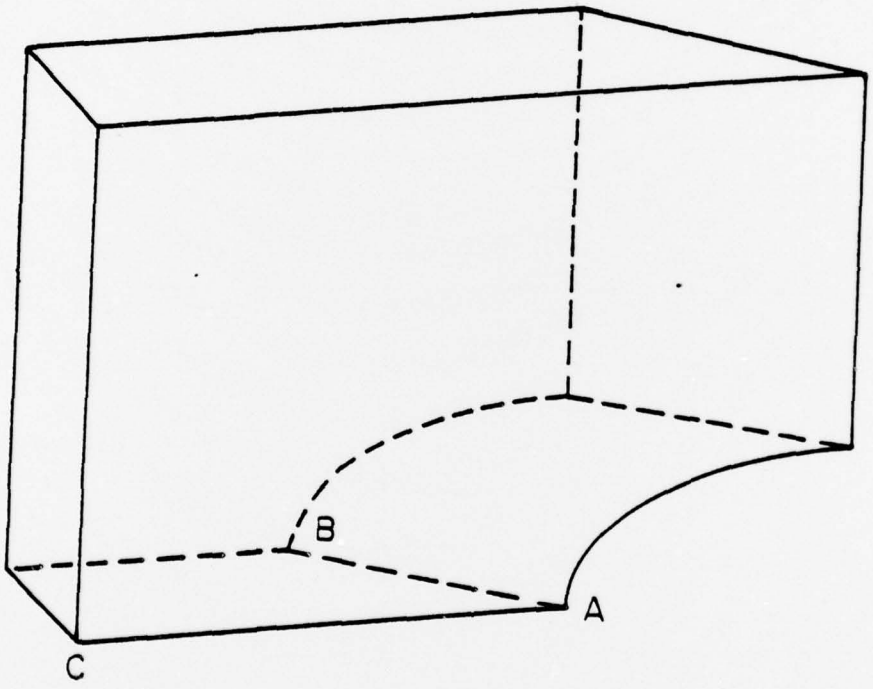

Figure 8. Quarter of Plate with 60° Skew Hole

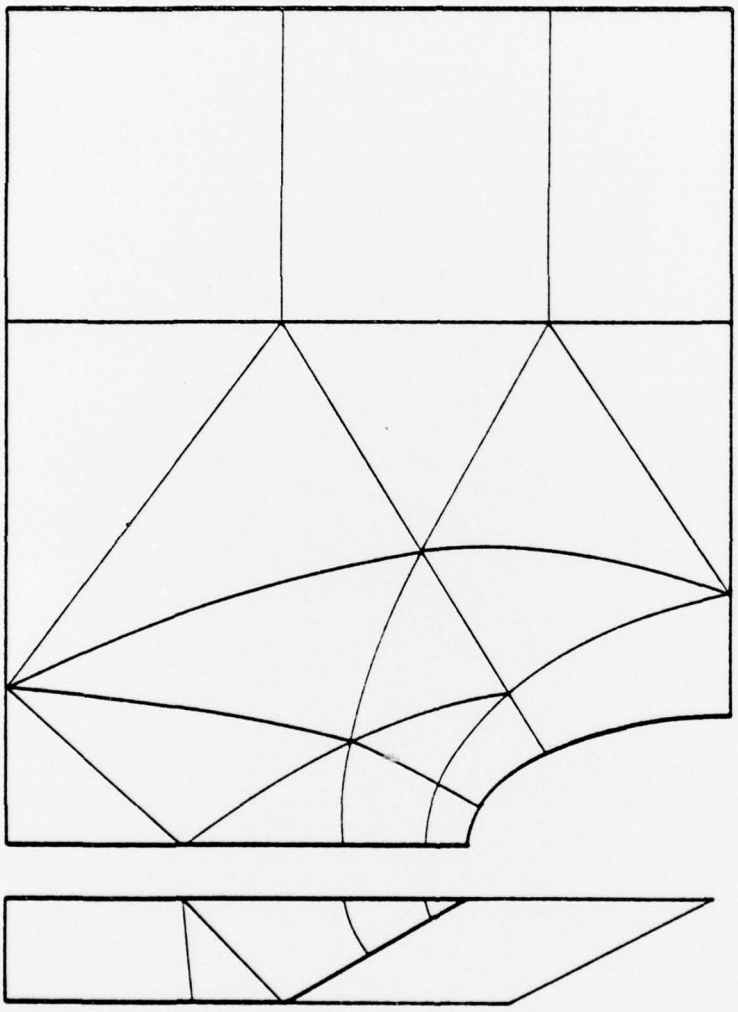

Figure 9. Surface Discretization of Quarter-Plate

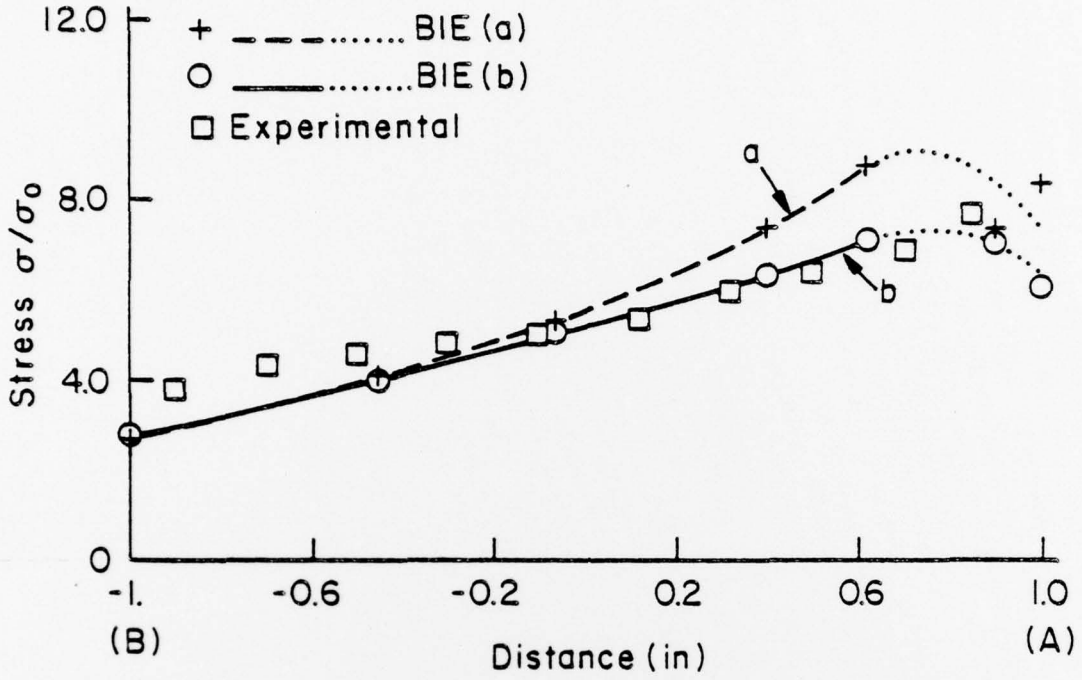

Figure 10. Variation of Normal Stress along Edge of Hole (Line AB)

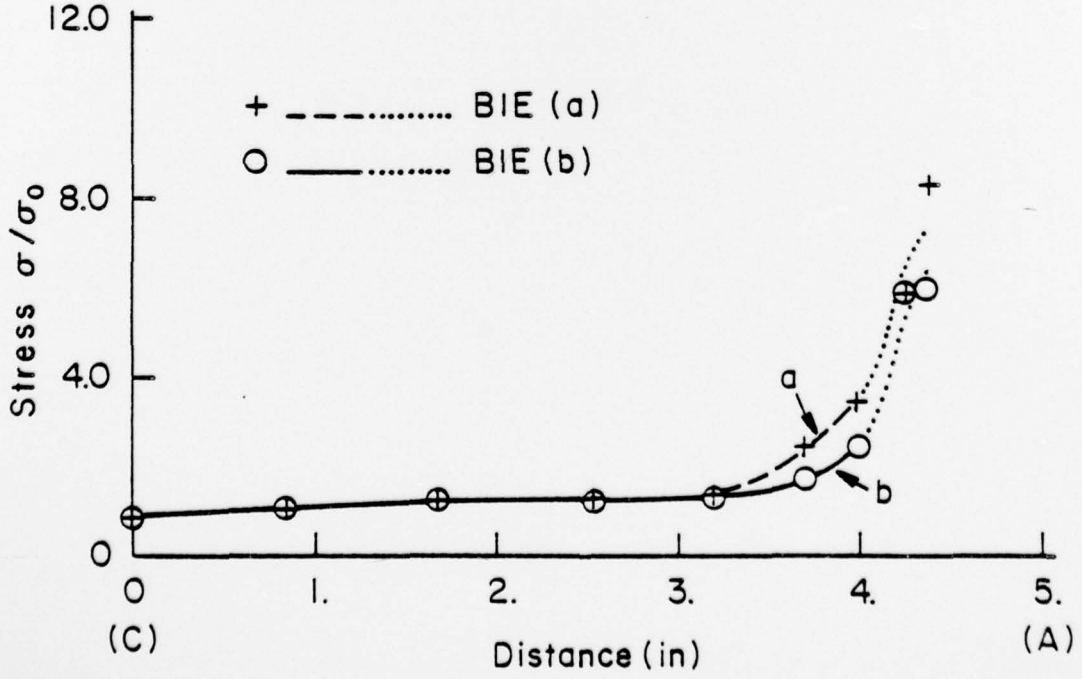

Figure 11. Variation of Normal Stress along Front Edge of Plate (Line AC)

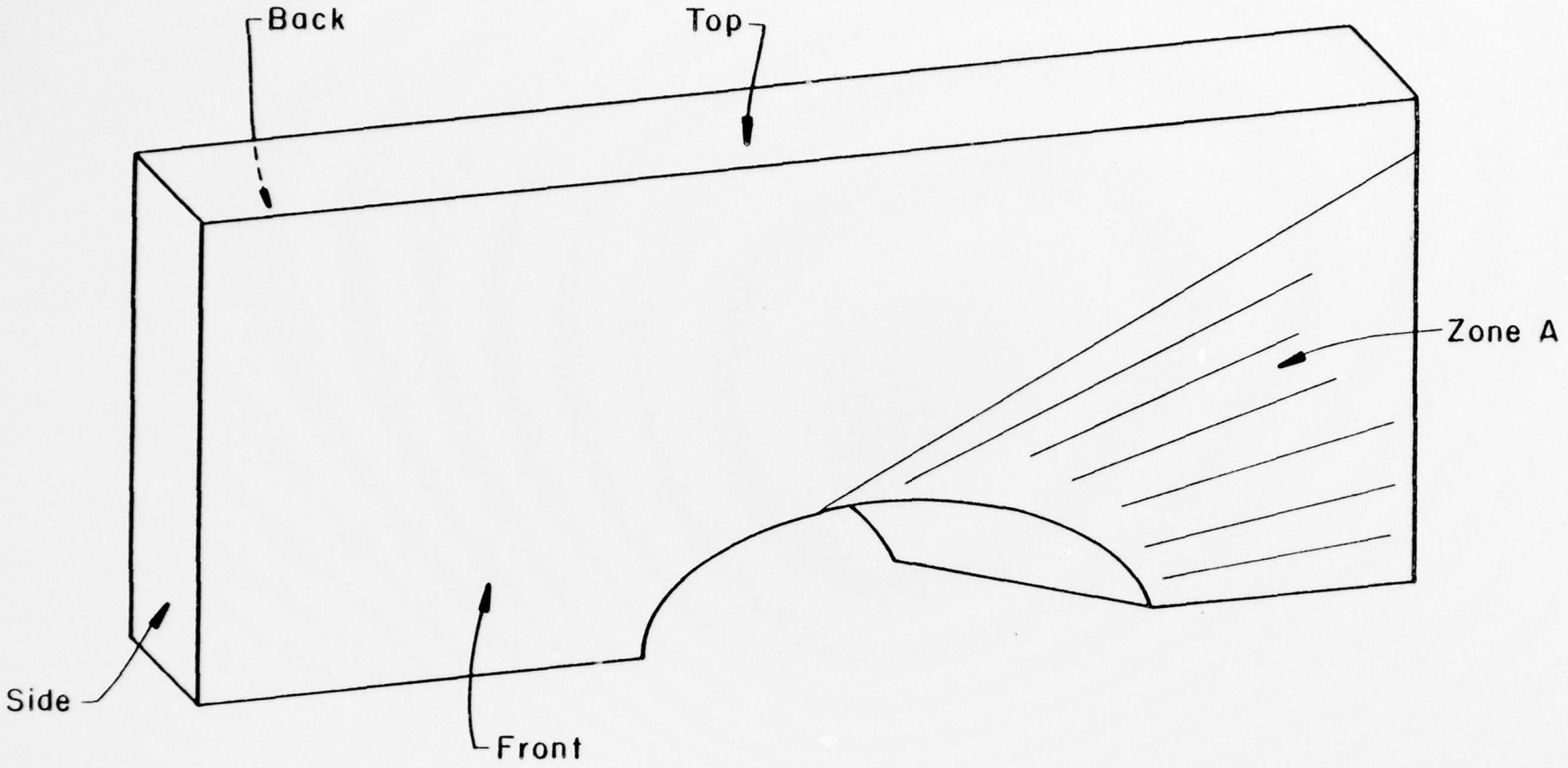

Figure 12. Half of Plate with Skew Hole, Showing Region of Mixing (Zone A)